

Plexcitonic Nanohybrids Based on Gold Nanourchins: The Role of the Capping Layer

Nicola Peruffo, Fabrizio Mancin,* and Elisabetta Collini*

Cite This: *J. Phys. Chem. C* 2021, 125, 19897–19905

Read Online

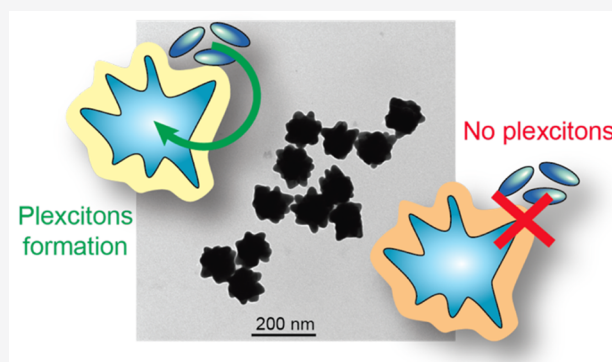
ACCESS |

Metrics & More

Article Recommendations

Supporting Information

ABSTRACT: Plexcitonic nanohybrids are plasmonic–excitonic novel materials whose peculiar properties are attracting considerable attention in photonics, solar cells, and sensing. These materials can be synthesized and characterized easily by assembling organic or inorganic dyes on plasmonic nanoparticles as support. However, the main factors controlling the assembly process and the occurrence of the plexcitonic coupling are still unclear. To fill this gap, in this work, we studied the plexciton coupling of 12 different dyes with a series of gold nanourchins with various coatings and sizes. Among 24 combinations tested, we observed the formation of plexcitonic hybrids only in five cases. Most of them had cyanine J-aggregates as excitonic counterparts. Stronger plexcitonic couplings were obtained when nanourchins were coated with an exchangeable citrate capping layer rather than a strong ionic thiols capping layer. We propose that the presence of a strongly bound capping layer, as in this latter case, reduces the effective volume available to the dyes.



INTRODUCTION

Plexcitonic nanohybrids, i.e., nanosystems characterized by plasmon–exciton couplings, have gained increasing attention over the last two decades for the fundamental interest they hold and for their potential applications. These nanomaterials are obtained by combining plasmonic substrates, such as nanostructured surfaces or nanoparticles, with excitonic systems like organic dyes, quantum dots, carbon nanotubes, or 2-dimensional transition-metal dichalcogenides, such as MoS₂ or WS₂.^{1–3} The peculiar optical properties of these materials might find application in photovoltaics,⁴ sensing,^{5,6} digital data storage,⁷ and in the broad field of photonics as a manner to control light–matter interactions at the nanoscale.^{1,3,8} However, plexciton behavior has to be wholly understood and characterized. As an example, the nature of excitations and the mechanisms of energy dissipation in these materials⁹ and phenomena as ultrafast coherences (Rabi oscillations),¹⁰ Bose–Einstein condensation,¹¹ and “induced transparency” (or Fano dip)^{12,13} are the object of several ongoing investigations.

Among the plasmonic systems, colloidal nanoparticles (NPs) are cheap and easy to prepare, being obtained through wet chemical syntheses. Thus, NP-supported plexcitonic nanohybrids inherit these advantages. On the other hand, the conjugation with the excitonic part is, at least conceptually, much simpler for plasmonic surfaces than for suspended NPs. In the first case, it is sufficient to deposit a film of the excitonic materials onto the plasmonic surface to obtain the necessary spatial proximity among the parts. Instead, the simple mixing

of NPs and the excitonic counterpart in solution does not ensure the formation of the wanted assembly. An attractive interaction between the two moieties is needed in this case. In most instances, NPs are coated with stabilizing species (ions, molecules, or polymers) to prevent their coalescence. This coating, also called the capping layer, clearly plays a crucial role in controlling the interaction between the NPs and the excitonic part. It influences the self-assembly process by determining the intermolecular forces at play, it affects the distances between NPs and dyes, and it can template different aggregation states of the bound excitonic moieties.¹⁴

Many works in the literature have investigated the main physicochemical parameters that regulate the plexcitonic coupling strength (see, for example, refs 9 and 15–21), but the role of the capping layer has never been examined in depth. Among the attractive interactions between the plasmonic and excitonic moieties enabled by the capping layer, electrostatic interactions appear to be the most commonly exploited in nanohybrid preparation.^{14,15,22} As an example, Mohankumar et al. demonstrated that repulsion between like charges prevented the assembly of gold nanorods and a cyanine dye and,

Received: July 1, 2021

Revised: August 5, 2021

Published: September 1, 2021



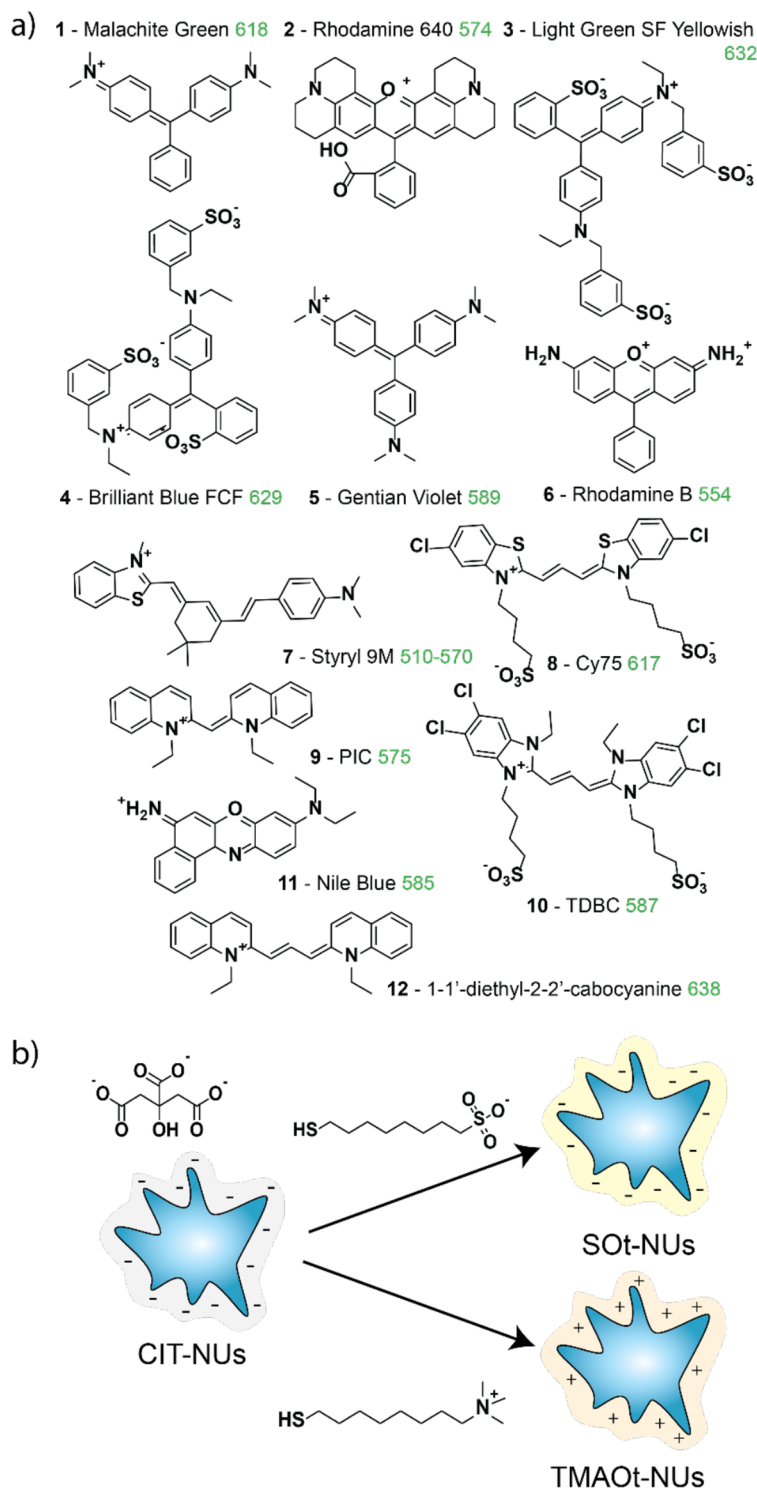


Figure 1. (a) Dyes considered in this study. For each dye, the main maximum absorption wavelength is reported in green. (b) Schematization of the different capping layers and their exchange process. CIT-NUs were exploited to study the role of direct dye–metal interactions, while SOT-NUS (TMAOt-NU) were employed to assess the role of noncovalent interactions between the capping layer and positively (negatively) charged dyes.

consequently, the plexciton formation.²³ In other cases, however, the capping layer does not provide specific interactions but acts as a weak stabilizer that can be exchanged (at least partially) by the dye molecules,^{24–27} as in the case of borohydride^{24,25} or citrate.^{26,27} This might result in direct metal–dye interactions.

With the aim of exploring in more detail the parameters which influence the formation of nanoparticle-based plexcitonic states in solution and to shed light on the effect of the capping layer, we prepared a library of nanohybrids by coupling gold nanourchins (NUs)²⁸ covered with different capping layers and several dyes featuring suitable photochemical properties. Our findings suggest that when the

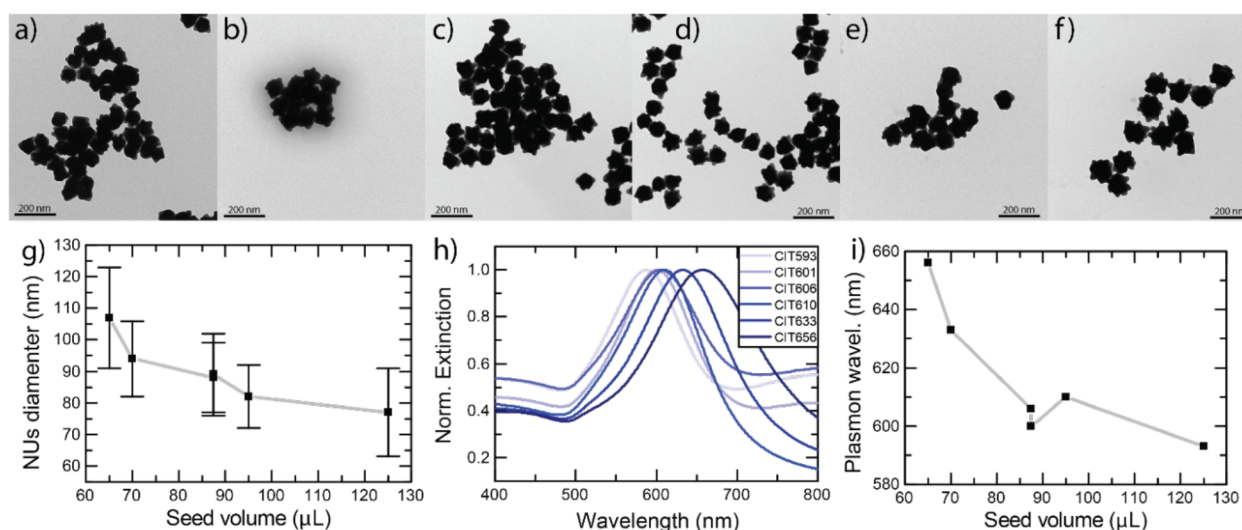


Figure 2. Characterization and functionalization of NUs. Each NU sample is labeled with an acronym where the first part denotes the capping layer (CIT, SOT, or TMAOt) and the second one the plasmon wavelength. (a–f) TEM images of CIT593, CIT601, CIT606, CIT610, CIT633, and CIT656, respectively (scale bar: 200 nm). (g) NU diameter as a function of the injected volume of seed solution (the seed solution has a concentration of 0.046 mg/mL). The diameters reported on the y axis are estimated as the central values of the NU size distribution fitted with a Gaussian function. The error bars correspond to the full-width half-maximum of the size distribution. (h) Normalized extinction spectra of CIT-NUs. (i) Wavelength of the maximum plasmonic resonance as a function of the injected volume of seeds solution.

capping layer allows for direct metal–dye interactions higher coupling values can be achieved than when noncovalent and electrostatic interactions are exploited. Moreover, we also found that the aggregation conditions of the dye molecules play an important role in the formation of plexitonic hybrids.

EXPERIMENTAL METHODS

Syntheses and Capping Layer Exchange of NUs. Gold nanourchins (NUs), similar to nanostars but with shorter tips, were prepared following a modified two-step protocol.²⁸ Briefly, gold seeds were synthesized using a modified Turkevich method and injected in a growth solution of HAuCl₄, hydroquinone, and sodium citrate. The use of hydroquinone as a reducing agent favors the anisotropic growth of the nanoparticles, resulting in the formation of the NUs. This synthetic protocol yielded NUs capped with citrate (CIT-NUs). CIT-NUs were used in this pristine form to be directly functionalized with the dyes or submitted to a subsequent ligand exchange. In this case, the CIT layer was replaced by strongly bound thiol derivatives: 8-trimethylammonium octylthiol (TMAOt), positively charged, or 8-sulfate octylthiol (SOT), negatively charged. Further information on the synthesis of NUs and of the TMAOt and SOT molecules is reported in the [Supporting Information](#).

NUs functionalized with SOT (SOT-NUs) were prepared as follows. NU batches were centrifuged for 8 min at 5000 rpm, and the supernatant was removed to eliminate most of the citrate and hydroquinone molecules free in solution. NUs were successively redispersed in 1 mL of ultrapure water and sonicated for 10 min. SOT molecules were added in a 100:1 SOT/NU ratio (we considered NUs as spheres of 100 nm diameter with a thiol footprint of 0.15 nm²). They were incubated for 90 min and successively purified twice from the impurities. Each purification step consisted of centrifugation (3 min, 10000 rpm), removal of the supernatant, and redispersion in 1 mL of ultrapure water. NUs capped with TMAOt (TMAOt-NUs) were prepared with a similar procedure. Pristine NUs batches were centrifuged (10 min, 5000 rpm)

and redispersed in 1 mL of 5 mM solution of NaNO₃ to prevent tips etching due to the joint action of trimethylammonium residues and bromide anions.²⁹ TMAOt molecules were added in a 800000:1 TMAOt/NU ratio. They were incubated overnight and successively purified from the impurities three times with the same protocol of SOT-NUs.

Preparation of the Nanohybrids. Typically, 100 μL of a 1 mM solution of dye were added to 500 μL of a solution of NUs whose concentration was set to have a plasmon peak extinction equal to 1, corresponding to a concentration of about 1.5 μg/mL. Only in the case of PIC, 1 μL of supersaturated solution of PIC in EtOH was added to 500 μL of NUs solution. The mixture was incubated overnight and then purified to remove the excess of dye. The purification protocol consisted of centrifugation (5 min, 7500 rpm), removal of the supernatant and redispersion in ultrapure water (0.4 mL).

Characterization. TEM analysis (100 measurements per NUs sample) was performed with a JEOL 300 PX electron microscope, and the collected images were analyzed with ImageJ software. A 10.0 μL portion of sample solution was dropcast onto a lacey carbon TEM grid and allowed to air-dry before TEM measurements. Extinction spectra were recorded with a Cary 5000 spectrophotometer, while a Zetasizer Nano ZS was used for Z potential measurements.

RESULTS

Design of the Nanohybrid Library. To build the library considered in this work, we started by identifying a wide enough number of organic dyes to be used as excitonic moieties. We selected 12 dyes (1–12, [Figure 1a](#)) belonging to the classes of triarylmethanes, rhodamines, cyanines, benzothiazoliums, and naphthoxaziniums. The following criteria drove the selection of the dyes. First, they all have strong absorptions in the 550–650 nm region of the visible spectrum, and therefore, they fulfill the resonance conditions necessary to establish an effective coupling with the majority of plasmonic colloidal nanoparticles.^{1,30–33} Second, they all have a net

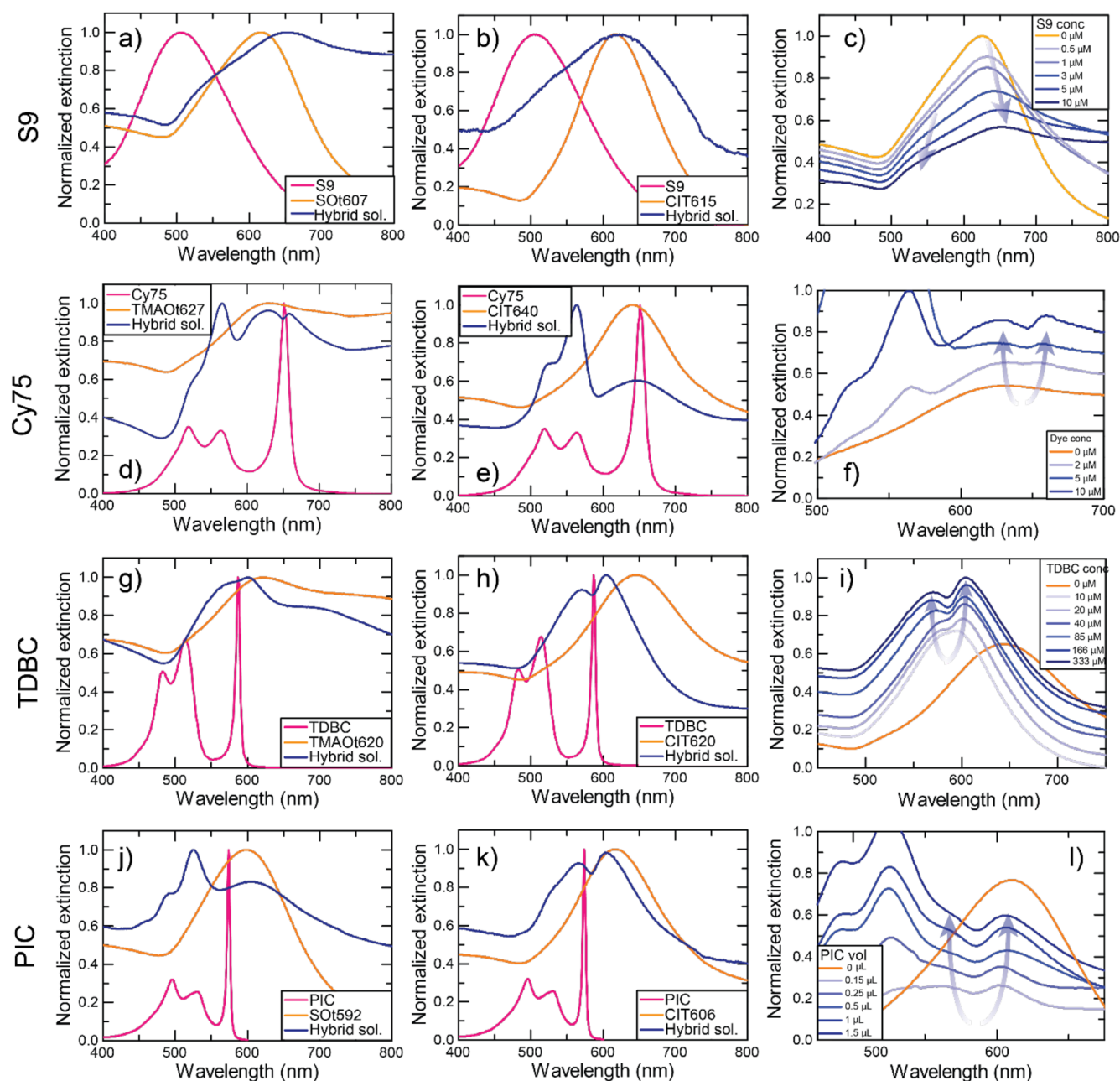


Figure 3. Normalized extinction spectra of dyes, NUs, and nanohybrid solutions (pink, orange, and dark blue lines, respectively) obtained using (a–c) S9, (d–f) Cy75, (g–i) TDBC, and (j–l) PIC as the organic dye. The first column (a, d, g, and j) refers to nanohybrids prepared with thiol-capped NUs exploiting noncovalent interactions; the second column (b, e, h, and k) relates to nanohybrids prepared with CIT-NUs controlling metal–dye interactions. The third column (c, f, j, and l) reports the typical concentration trend of Ω_R , which increases as the dye concentration is raised.

charge, which can provide an essential contribution to the interaction with the plasmonic nanoparticles. Both negatively and positively charged molecules were included. About half of the molecules selected are known to form H- or J-aggregates (Table S1). Indeed, the high transition dipole moments and the narrow bandwidths typical of the J-aggregate absorption bands make them particularly suited for the formation of plexitons,¹⁷ as proven by the vast wealth of examples available in the literature (see, for instance, refs 14, 15, 24, 26, and 34–36). Instead, the formation of plexitons with molecular excitations coming from organic molecules in the monomeric form is seldom observed with nanoparticles dispersed in

solution.^{14,23,37–40} On the contrary, to the best of our knowledge, there is no report of formation of plexitons with colloidal NPs dispersed in solution and H-aggregates. Therefore, the dyes have also been selected in view of exploring the conditions for the possible plexiton formation with non-aggregated molecules, J-aggregates, and H-aggregates.

As plasmonic materials, gold NUs, i.e., short-tipped gold nanostars, were chosen for two main reasons. First, as for nanostars, the tip plasmon is easily tunable from 550 nm to the infrared region by controlling the synthetic conditions, and this guarantees an adequate overlap with the dyes' absorption.²⁸ Second, the NU structure features strong electric fields at the

tips, which should positively contribute to the establishment of strong couplings.⁴¹

We analyzed NUs coated with three different capping layers in order to have insights about different dye–NU interactions. First, NUs stabilized with the weak capping agent citrate (CIT-NUs)^{24–27} were studied, with the aim of understanding to what extent the possibility of a (partial) exchange of CIT with dye molecules could lead to direct metal–dye interaction. We also considered NUs covered with the cationic 8-trimethylammonium octylthiol (TMAOt-NUs) and the anionic 8-sulfate octylthiol (SOT-NUs) (Figure 1b). In both cases, different from CIT-NUs, the capping molecules are strongly attached to the metal surface and the dye molecules can thus interact with the NUs only through electrostatic interactions with the sulfate or ammonium groups or through hydrophobic interaction with the alkyl portion of the coating layer.

Preparation of the NUs and the Nanohybrids. NUs with different sizes were prepared according to a previously reported protocol as described in the *Experimental Methods*.²⁸ In this protocol, the size and plasmonic properties of the NUs are determined by the amount (volume) of seed solution injected into the growth solution. Transmission electron microscopy (TEM) micrographs of six samples and their size analysis are reported in Figure 2a–f and Figure S1a–f, respectively. As expected, the size of NUs decreases by increasing the number of seeds (Figure 2g). The extinction spectra of the NUs (Figure 2h) are characterized by two plasmon resonances: a first weak signal at about 520 nm is due to the plasmon of the core and a second more intense band above 550 nm is instead attributed to the plasmon of the tips.⁴¹ The maximum of this second band is sensitive to the size of the NUs, and therefore, it depends on the volume of seed solution injected during the synthesis: a blue shift is recorded for increasing volumes of seed solution (Figure 2i and Figure S2).

Pristine NUs prepared with this protocol are capped with citrate (CIT-NUs). We then prepared TMAOt-NUs and SOT-NUs using capping-exchange procedures (see the *Experimental Methods*). The effective surface charge of the NUs covered with the three different capping layers was verified through Z-potential measurements (see Figure S3).

Eventually, we prepared the nanohybrid library by mixing each of the 12 dyes with (i) CIT-NUs and (ii) with the NUs capped with the thiol of opposite charge. Twenty-four combinations were thus obtained. Spectroscopic analysis after 1 day of incubation revealed the increase significant plexcitonic coupling only in five cases. The plexciton formation can be monitored looking at the appearance of a transparency dip in the plasmon resonance along with the maximum absorbance of the excitonic moiety.³⁰ The coupling strength can then be quantitatively evaluated from the Rabi splitting energy Ω_R , estimated from the energy distance between the two plexciton resonances formed in the excitation spectra of the nanohybrids.^{1,2,30}

Here, we describe the properties of these five successful examples of plexciton formation, classified in terms of the aggregation state of the dye and the nature of the interactions between dye and NUs (noncovalent interaction or direct metal–dye interaction).

Plexcitonic Nanohybrids with Nonaggregated Molecules: Styryl 9M. Dyes 1–7, including styryl 9 M (S9, 7), triarylmethanes, and rhodamines, do not form aggregates when dissolved in water. Among them, we observed plexcitonic resonances only in nanohybrids prepared with cationic S9 and

SOT-NUs (Figure 3a). To the best of our knowledge, this is the first time that a plexciton with S9 is reported. S9 is a solvatochromic dye: its maximum absorption peak undergoes a red-shift when the polarity of the solvent is decreased.⁴² As an example, the absorption maximum is found at 510 nm in a 99:1 water/acetone solution and at 570 nm in acetone solution (Table S1). The extinction spectrum of S9/CIT-NUs hybrids appeared just as the sum of the spectra of the single components, and therefore, no relevant interactions between the NUs and the dyes are established in these conditions (Figure 3b). On the contrary, in the case of S9/SOT-NUs, two peaks could be detected at about 652 and 526 nm, which we attributed to the formation of two plexciton resonances. From the energy separation among these two peaks a Rabi splitting (Ω_R) of ~ 450 meV can be estimated. This assignment is supported by the fact that the distance between the two peaks increased by increasing the S9 concentration (Figure 3c). Indeed, this behavior is typical of plexcitonic resonances, whose Rabi splitting is proportional to the square of the number of coupled molecules.^{16,43–45} It is remarkable that in these nanohybrids the plexcitonic resonance forms even if the plasmon band of NUs (625 nm) poorly overlaps with the dye's absorption band. We suggest that the dye, embedded in the nanoparticle coating layer, experiences a low polarity environment and red-shifts its absorbance peak, reducing the detuning and allowing an effective plexcitonic coupling. TEM analysis of SOT-NUs before and after the addition of S9 did not reveal any structural modification in the NUs morphology (Figure S4a,b).

Plexcitonic Nanohybrids with J-Aggregating Molecules. Dyes 8–10, all belonging to the cyanine family, easily form J-aggregates in the appropriate ionic strength, concentration, or temperature conditions.^{46,47} For all these molecules, we observed the formation of plexcitons after conjugation with the NUs.

Cy75 (8) is an anionic dye that aggregates in water solutions at high ionic strength values (NaCl 0.05 mM, Figure 3d).⁴⁸ This dye in its J-aggregate form has already been employed to prepare plexcitonic materials in the form of film-coupled nanocube cavities.⁴⁸ When Cy75 was mixed with CIT-NUs, it did not produce plexcitonic resonances nor aggregate formation (Figure 3e). Instead, in the presence of TMAOt-NUs the typical features associated with the formation of plexcitonic resonances appeared (Figure 3d): a dip in correspondence of the excitonic band of Cy75 J-aggregates (650 nm) and two side peaks (629 and 658 nm, $\Omega_R \approx 85$ meV).^{20,23} As for S9, the concentration trend supports the attribution of these two new peaks to plexciton resonances (Figure 3f). Also in this case, the TEM analysis of TMAOt-NUs before and after the addition of Cy75 did not reveal any significant structural modification (Figures S4c,d).

TDBC (10) is an anionic dye well-known for the formation of J-aggregates at high concentrations^{49,50} and it is often used for preparing plexcitonic materials; see, for instance, refs 18, 20, 26, and 51. With this dye, we observed the formation of plexcitonic resonances independently on the NUs capping layer (Figures 3g,h), although with slightly different coupling values: we estimated $\Omega_R = 120$ meV for TDBC/CIT-NUs and 95 meV for TDBC/TMAOt-NUs. Also in this case, the dependence of the Rabi splitting on the dye concentration was confirmed (Figure 3i). Different from the two previously described systems, the TEM images of CIT-NUs before and after the addition of TDBC revealed the smoothing of the tips after the functionalization with the dye (Figures 4a,b), which

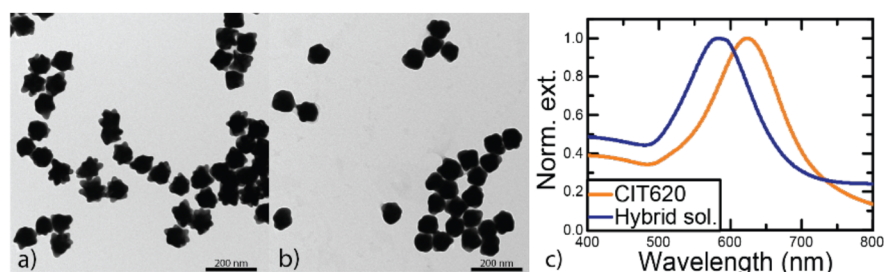


Figure 4. TEM images of CIT620 (a) before and (b) after TDBC addition (scale bar: 200 nm). (c) Extinction spectra of CIT620 before (orange line) and after (dark blue line) TDBC addition (final TDBC concentration: 10 μ M).

induced a blueshift of the absorption band associated with the tip plasmon, even at low TDBC concentration (Figure 4c and Figure 3h). This reshaping is clear proof that TDBC exchanged CIT molecules on the NU surface, establishing a direct interaction with the metal surface.

PIC (9) is a positively charged dye (Figure 1a) that aggregates at high temperature (85 $^{\circ}$ C) and in high ionic strength conditions (see refs 49 and 50). With TDBC, it is one of the most used dyes for preparing plexcitonic materials (see, for instance, refs 17 and 52–54). We found that when nonaggregated PIC to SOT-NUs (Figure 3j) and CIT-NUs (Figures 3k,l) were added, the plexcitonic coupling was established only with the latter, with a Rabi splitting of 130 meV. No plexciton formation or dye aggregation were observed in the presence of SOT-NUs. We also tried to prepare the nanohybrids by adding preaggregated PIC to the NUs. In both cases, a broad and intense band above 700 nm, due to NUs aggregation, dominates the extinction spectra of the hybrids (Figure S5). Despite that, plexciton resonances appeared again only with CIT-NUs. In light of these results, it can be concluded that the inability of SOT-NUs to produce plexcitonic coupling with PIC is not related to the capability of templating the dye aggregation. As for TDBC/CIT-NUs nanohybrids, we noted a reshaping of CIT-NUs (Figures S4e,f) and a blueshift of the plasmon peak (see, for instance, Figure 3k) after the addition of the dye molecules. Therefore, also in this case, the formation of direct interactions between the dye and the metal surface consequent to CIT exchange could be established.

Nanohybrids with H-Aggregating Molecules. Nile blue (11), which usually is present in solution as a monomer, formed H-aggregates in the presence of SOT-NUs (Figure S6a), as also reported for anionic SnO_2 and SiO_2 nanoparticles, but no plexciton resonance was observed both with CIT- and SOT-NUs.⁵⁵ 1,1'-Diethyl-2,2'-carbocyanine (12) typically forms H-aggregates.⁵⁶ Here, we neither observed the nucleation of H-aggregates onto NUs surface, nor any plexciton formation both with CIT- and SOT-NUs. However, we observed the blueshift of the tip plasmon, likely due to the tips' smoothing, in the case of CIT-NUs (Figure S6b).

DISCUSSION

The results reported in this work allowed building the first example of a library of plexcitonic materials based on colloidal NUs. To the best of our knowledge, similar systems have been studied so far only by Melnikau et al., who reported a preliminary investigation on plexcitons promoted by the coupling of gold nanostars and two cyanine dyes.³⁵ Our deep and complete characterization of these systems definitely proved the high suitability of NUs to couple with organic dyes.

As mentioned, the easy tunability of the tip plasmon and the enhancement of the electric fields at the tips make these structures particularly suited in view of achieving strong coupling with organic dyes and the effective formation of hybrid plexcitonic resonances.

Despite the relatively wide range of families of organic dyes taken into consideration, cyanine dyes were revealed to be the most effective in the formation of plexcitons, especially in their J-aggregate form, confirming a trend already widely established in the literature.

More interesting are the different behaviors manifested by the cyanine molecules in the coupling with NUs stabilized by different capping agents. Two classes of capping agents have been considered. On the one hand, we found evidence that, with CIT-capped NUs, the dyes can establish direct interactions with the metal surface after the (partial) exchange of the capping molecules. The reshaping of the NUs' tips after the functionalization with the dye, as proved by the TEM analysis and the blue shift of the plasmonic resonance, is a clear indication of a partial exchange of the CIT by the cyanine molecules and the establishment of direct metal–dye interactions. On the other hand, in the case of thiol-capped NUs negatively or positively charged the direct interaction is not possible, as confirmed by the absence of any reshaping or plasmon shifts, and the association between the dyes and the NUs is due to electrostatic interactions with dyes of opposite charge and possibly to hydrophobic interactions between the nonpolar portions of the dyes and the inner alkyl part of the capping layer.

We found that while TDBC interacts both with thiol-capped NUs and CIT-capped NUs to form plexciton hybrids, PIC can form plexcitons only with CIT-NUs and Cy75 only with thiol-capped NUs. These findings confirm that the interaction between the metal nanostructures and the organic dye molecules in plexciton formation is strongly modulated by the nature of the capping agent, which therefore requires a careful evaluation.

In particular, the TDBC case allows the direct comparison of the effectiveness of indirect noncovalent and direct metal–dye interactions by examining the TMAOt-NUs/TDBC and CIT-NUs/TDBC hybrids. Stronger coupling is observed in CIT-NUs ($\Omega_R \approx 120$ meV) than in TMAOt-NUs ($\Omega_R \approx 95$ meV). It is likely that the establishment of direct interactions reduces the distance between the dye and the surface of the nanoparticles and increases the number of dyes within the effective volume (i.e., the volume where the NUs plasmon enhance the electromagnetic field).^{57,58} This trend is also confirmed by CIT-NUs/PIC ($\Omega_R \approx 130$ meV) and TMAOt-NUs/Cy75 ($\Omega_R \approx 85$ meV), although the molecules compared are different.

Indeed, in the interplay between dye–nanoparticle interactions and the formation of plexcitonic hybrids, the properties of dye molecules must be kept into account. The Cy75 dye, whose structure is similar to that of TDBC, forms a plexcitonic hybrid only with TMAOt-NUs but not with CIT-NUs. With respect to TDBC, Cy75 features benzothiazole rather than benzimidazole groups and lacks two chlorine atoms at the 6,6' positions and the ethyl groups at the 1,1' positions of the heterocycles. These structural differences explain its lower tendency to aggregation in water solutions^{46,47} and might also be responsible for its reduced capability of exchanging CIT molecules and forming aggregates on the metal surface.

We also found that S9 is the only nonaggregating dye, among the other seven molecules tested, capable of producing plexcitonic resonances. It is probably not a case that S9 is the only species presenting an elongated structure with a polymethine chain connecting two (hetero) cyclic terminal groups, very similar to the cyanine structure. Moreover, the lower polarity environment provided by the capping layer also seems to favor the plexcitonic coupling by reducing the detuning between the molecular and the plasmonic resonances.

These findings suggest that mere electrostatic forces between oppositely charged capping molecules and organic dyes, while important,²⁰ are not enough to establish a strong coupling. Most likely, a delicate balance between electrostatic, dispersion, and hydrophobic forces both between dyes and between dyes and capping molecules determine the final coupling regime.

CONCLUSIONS

In conclusion, in this study we systematically explored the formation of plexcitonic resonances in a library of colloidal hybrids prepared by coupling gold nanourchins and different dyes. The attention was focused particularly on the still underexplored role of the capping layer in mediating the interaction and the coupling between the organic dye and the plasmonic substrate.

Beyond providing new examples of plexcitonic hybrids never reported before, we found that the nature of the capping layer is crucial to determine the establishment of the coupling between dyes and plasmonic substrate, which is the result of a delicate and complex balance between a wealth of various dye–dye and dye–capping molecules interactions: electrostatic, dispersive, and hydrophobic forces.

Our findings suggest that, at least with cyanine and cyanine-like molecules, stronger couplings are achieved when a direct metal–dye interaction can be established after the exchange of capping molecules by dye molecules. These insights shed light on a still unexplored aspect of the plasmon–exciton interactions and open new perspectives for the design of novel and performative plexcitonic nanohybrids.

ASSOCIATED CONTENT

Supporting Information

The Supporting Information is available free of charge at <https://pubs.acs.org/doi/10.1021/acs.jpcc.1c05862>.

Table of dyes (1–12) features and their full names; synthetic procedure of NUs; TEM histogram of NUs reported in Figure 2; synthesis and characterization of TMAOt and SOT molecules; Z potential measurements and extinction spectra of uncoupled CIT-NUs, SOT-NUs, and TMAOt-NUs; TEM images of NUs before

and after S9, Cy75, and TDBC addition; extinction spectra of the nanohybrids obtained with preaggregated PIC; extinction spectra of nanohybrids with H-aggregates (PDF)

AUTHOR INFORMATION

Corresponding Authors

Elisabetta Collini – Department of Chemical Sciences and Padua Quantum Technologies Research Center, c/o Department of Chemical Sciences, University of Padova, 35131 Padova, Italy; orcid.org/0000-0002-1019-9100; Email: elisabetta.collini@unipd.it

Fabrizio Mancin – Department of Chemical Sciences, University of Padova, 35131 Padova, Italy; orcid.org/0000-0003-0786-0364; Email: fabrizio.mancin@unipd.it

Author

Nicola Peruffo – Department of Chemical Sciences, University of Padova, 35131 Padova, Italy

Complete contact information is available at: <https://pubs.acs.org/10.1021/acs.jpcc.1c05862>

Notes

The authors declare no competing financial interest.

ACKNOWLEDGMENTS

This research is funded by a “CQ-TECH” STARS grant 2019 (2019-UNPD0Z9-0166571) from the University of Padova.

ABBREVIATIONS

CIT-NUs, NUs capped with citrate; NPs, colloidal nanoparticles; NUs, gold nanourchins; SOT, 8-sulfate octylthiol molecule; SOT-NUs, NUs capped with SOT; S9, styryl 9M; TEM, transmission electron microscopy; TMAOt, 8-trimethylammonium octylthiol molecule; TMAOt-NUs, NUs capped with TMAOt; Ω_R , Rabi splitting

REFERENCES

- (1) Marquier, F.; Sauvan, C.; Greffet, J.-J. Revisiting Quantum Optics with Surface Plasmons and Plasmonic Resonators. *ACS Photonics* **2017**, *4*, 2091–2101.
- (2) Baranov, D. G.; Wersäll, M.; Cuadra, J.; Antosiewicz, T. J.; Shegai, T. Novel Nanostructures and Materials for Strong Light-Matter Interactions. *ACS Photonics* **2018**, *5*, 24–42.
- (3) Hugall, J. T.; Singh, A.; van Hulst, N. F. Plasmonic Cavity Coupling. *ACS Photonics* **2018**, *5*, 43–53.
- (4) Nan, F.; Ding, S. J.; Ma, L.; Cheng, Z. Q.; Zhong, Y. T.; Zhang, Y. F.; Qiu, Y. H.; Li, X.; Zhou, L.; Wang, Q. Q. Plasmon Resonance Energy Transfer and Plexcitonic Solar Cell. *Nanoscale* **2016**, *8*, 15071–15078.
- (5) Hazra, B.; Das, K.; Chakraborty, S.; Das Verma, M. S.; Devi, M. M.; Katiyar, N. K.; Biswas, K.; Senapati, D.; Chandra, M. Hollow Gold Nanoprism as Highly Efficient “Single” Nanotransducer for Surface-Enhanced Raman Scattering Applications. *J. Phys. Chem. C* **2016**, *120*, 25548–25556.
- (6) Walters, C. M.; Pao, C.; Gagnon, B. P.; Zamecnik, C. R.; Walker, G. C. Bright Surface-Enhanced Raman Scattering with Fluorescence Quenching from Silica Encapsulated J-Aggregate Coated Gold Nanoparticles. *Adv. Mater.* **2018**, *30*, 1705381.
- (7) Schwartz, T.; Hutchison, J. A.; Genet, C.; Ebbesen, T. W. Reversible Switching of Ultrastrong Light-Molecule Coupling. *Phys. Rev. Lett.* **2011**, *106*, 1–4.
- (8) Manuel, A. P.; Kirkey, A.; Mahdi, N.; Shankar, K. Plexcitonics-Fundamental Principles and Optoelectronic Applications. *J. Mater. Chem. C* **2019**, *7*, 1821–1853.

- (9) Finkelstein-Shapiro, D.; Mante, P.-A.; Sarisozen, S.; Wittenbecher, L.; Minda, I.; Balci, S.; Pullerits, T.; Zigmantas, D. Understanding Radiative Transitions and Relaxation Pathways in Plexcitons. *Chem.* **2021**, *7*, 1092–1107.
- (10) Vasa, P.; Wang, W.; Pomraenke, R.; Lammers, M.; Maiuri, M.; Manzoni, C.; Cerullo, G.; Lienau, C. Real-Time Observation of Ultrafast Rabi Oscillations between Excitons and Plasmons in Metal Nanostructures with J-Aggregates. *Nat. Photonics* **2013**, *7*, 128–132.
- (11) Kéna-Cohen, S.; Forrest, S. R. Room-Temperature Polariton Lasing in an Organic Single-Crystal Microcavity. *Nat. Photonics* **2010**, *4*, 371–375.
- (12) Leng, H.; Szychowski, B.; Daniel, M.-C.; Pelton, M. Strong Coupling and Induced Transparency at Room Temperature with Single Quantum Dots and Gap Plasmons. *Nat. Commun.* **2018**, *9*, 4012.
- (13) Murata, N.; Hata, R.; Ishihara, H. Crossover between Energy Transparency Resonance and Rabi Splitting in Antenna-Molecule Coupled Systems. *J. Phys. Chem. C* **2015**, *119*, 25493–25498.
- (14) Peruffo, N.; Gil, G.; Corni, S.; Mancin, F.; Collini, E. Selective Switching of Multiple Plexcitons in Colloidal Materials: Directing the Energy Flow at the Nanoscale. *Nanoscale* **2021**, *13*, 6005–6015.
- (15) Fofang, N. T.; Park, T. H.; Neumann, O.; Mirin, N. A.; Nordlander, P.; Halas, N. J. Plexcitonic Nanoparticles: Plasmon-Exciton Coupling in Nanoshell-J-Aggregate Complexes. *Nano Lett.* **2008**, *8*, 3481–3487.
- (16) Chikkaraddy, R.; de Nijs, B.; Benz, F.; Barrow, S. J.; Scherman, O. A.; Rosta, E.; Demetriadou, A.; Fox, P.; Hess, O.; Baumberg, J. J. Single-Molecule Strong Coupling at Room Temperature in Plasmonic Nanocavities. *Nature* **2016**, *535*, 127.
- (17) Thomas, R.; Thomas, A.; Pullanchery, S.; Joseph, L.; Somasundaran, S. M.; Swathi, R. S.; Gray, S. K.; Thomas, K. G. Plexcitons: The Role of Oscillator Strengths and Spectral Widths in Determining Strong Coupling. *ACS Nano* **2018**, *12*, 402–415.
- (18) Kumar, M.; Dey, J.; Verma, M. S.; Chandra, M. Nanoscale Plasmon-Exciton Interaction: The Role of Radiation Damping and Mode-Volume in Determining Coupling Strength. *Nanoscale* **2020**, *12*, 11612–11618.
- (19) Hendel, T.; Krivenkov, V.; Sánchez-Iglesias, A.; Grzelczak, M.; Rakovich, Y. P. Strongly Coupled Exciton-Plasmon Nanohybrids Reveal Extraordinary Resistance to Harsh Environmental Stressors: Temperature, PH and Irradiation. *Nanoscale* **2020**, *12*, 16875–16883.
- (20) Das, K.; Dey, J.; Verma, M. S.; Kumar, M.; Chandra, M. Probing the Role of Oscillator Strength and Charge of Exciton Forming Molecular J-Aggregates in Controlling Nanoscale Plasmon-Exciton Interactions. *Phys. Chem. Chem. Phys.* **2020**, *22*, 20499–20506.
- (21) Yoshida, A.; Yonezawa, Y.; Kometani, N. Tuning of the Spectroscopic Properties of Composite Nanoparticles by the Insertion of a Spacer Layer: Effect of Exciton-Plasmon Coupling. *Langmuir* **2009**, *25*, 6683–6689.
- (22) Yoshida, A.; Uchida, N.; Kometani, N. Synthesis and Spectroscopic Studies of Composite Gold Nanorods with a Double-Shell Structure Composed of Spacer and Cyanine Dye J-Aggregate Layers. *Langmuir* **2009**, *25*, 11802–11807.
- (23) Mohankumar, M.; Unnikrishnan, M.; Naidu, G. N.; Somasundaran, S. M.; Ajaykumar, M. P.; Swathi, R. S.; Thomas, K. G. Finding the Needle in a Haystack: Capturing Veiled Plexcitonic Coupling through Differential Spectroscopy. *J. Phys. Chem. C* **2020**, *124*, 26387–26395.
- (24) Kometani, N.; Tsubonishi, M.; Fujita, T.; Asami, K.; Yonezawa, Y. Preparation and Optical Absorption Spectra of Dye-Coated Au, Ag, and Au/Ag Colloidal Nanoparticles in Aqueous Solutions and in Alternate Assemblies. *Langmuir* **2001**, *17*, 578–580.
- (25) Wiederrecht, G. P.; Wurtz, G. A.; Hranisavljevic, J. Coherent Coupling of Molecular Excitons to Electronic Polarizations of Noble Metal Nanoparticles. *Nano Lett.* **2004**, *4*, 2121–2125.
- (26) Balci, S. Ultrastrong Plasmon-Exciton Coupling in Metal Nanoprisms with J-Aggregates. *Opt. Lett.* **2013**, *38*, 4498.
- (27) Krivenkov, V.; Samokhvalov, P.; Nabiev, I.; Rakovich, Y. P. pH-Sensing Platform Based on Light-Matter Coupling in Colloidal Complexes of Silver Nanoplates and J-Aggregates. *J. Phys. Chem. C* **2021**, *125*, 1972–1979.
- (28) Li, J.; Wu, J.; Zhang, X.; Liu, Y.; Zhou, D.; Sun, H.; Zhang, H.; Yang, B. Controllable Synthesis of Stable Urchin-like Gold Nanoparticles Using Hydroquinone to Tune the Reactivity of Gold Chloride. *J. Phys. Chem. C* **2011**, *115*, 3630–3637.
- (29) Rodríguez-Lorenzo, L.; Romo-Herrera, J. M.; Pérez-Juste, J.; Alvarez-Puebla, R. A.; Liz-Marzán, L. M. Reshaping and LSPR Tuning of Au Nanostars in the Presence of CTAB. *J. Mater. Chem.* **2011**, *21*, 11544–11549.
- (30) Törmä, P.; Barnes, W. L. Strong Coupling between Surface Plasmon Polaritons and Emitters: A Review. *Rep. Prog. Phys.* **2015**, *78*, 13901.
- (31) Cao, E.; Lin, W.; Sun, M.; Liang, W.; Song, Y. Exciton-Plasmon Coupling Interactions: From Principle to Applications. *Nanophotonics* **2018**, *7*, 145–167.
- (32) Ebbesen, T. W. Hybrid Light-Matter States in a Molecular and Material Science Perspective. *Acc. Chem. Res.* **2016**, *49*, 2403–2412.
- (33) Kolaric, B.; Maes, B.; Clays, K.; Durt, T.; Caudano, Y. Strong Light-Matter Coupling as a New Tool for Molecular and Material Engineering: Quantum Approach. *Adv. Quantum Technol.* **2018**, *1*, 1800001.
- (34) Balci, F. M.; Sarisozen, S.; Polat, N.; Balci, S. Colloidal Nanodisk Shaped Plexcitonic Nanoparticles with Large Rabi Splitting Energies. *J. Phys. Chem. C* **2019**, *123*, 26571–26576.
- (35) Melnikau, D.; Savateeva, D.; Susha, A.; Rogach, A. L.; Rakovich, Y. P. Plasmon-Exciton Strong Coupling in a Hybrid System of Gold Nanostars and J-Aggregates. *Nanoscale Res. Lett.* **2013**, *8*, 134.
- (36) Melnikau, D.; Govyadinov, A. A.; Sánchez-Iglesias, A.; Grzelczak, M.; Liz-Marzán, L. M.; Rakovich, Y. P. Strong Magneto-Optical Response of Nonmagnetic Organic Materials Coupled to Plasmonic Nanostructures. *Nano Lett.* **2017**, *17*, 1808–1813.
- (37) Nan, F.; Zhang, Y. F.; Li, X.; Zhang, X. T.; Li, H.; Zhang, X.; Jiang, R.; Wang, J.; Zhang, W.; Zhou, L.; et al. Unusual and Tunable One-Photon Nonlinearity in Gold-Dye Plexcitonic Fano Systems. *Nano Lett.* **2015**, *15*, 2705–2710.
- (38) Ni, W.; Yang, Z.; Chen, H.; Li, L.; Wang, J. Coupling between Molecular and Plasmonic Resonances in Freestanding Dye-Gold Nanorod Hybrid Nanostructures. *J. Am. Chem. Soc.* **2008**, *130*, 6692–6693.
- (39) Choi, Y.; Kang, T.; Lee, L. P. Plasmon Resonance Energy Transfer (PRET)-Based Molecular Imaging of Cytochrome C in Living Cells. *Nano Lett.* **2009**, *9*, 85–90.
- (40) Ni, W.; Chen, H.; Su, J.; Sun, Z.; Wang, J.; Wu, H. Effects of Dyes, Gold Nanocrystals, PH, and Metal Ions on Plasmonic and Molecular Resonance Coupling. *J. Am. Chem. Soc.* **2010**, *132*, 4806–4814.
- (41) Senthil Kumar, P.; Pastoriza-Santos, I.; Rodríguez-González, B.; Javier García De Abajo, F.; Liz-Marzán, L. M. High-Yield Synthesis and Optical Response of Gold Nanostars. *Nanotechnology* **2008**, *19*, 015606.
- (42) Yordanova, S.; Petkov, I.; Stoyanov, S. Solvatochromism of Homodimeric Styryl Pyridinium Salts. *J. Chem. Technol. Metall.* **2014**, *49*, 601–609.
- (43) Dicke, R. H. Coherence in Spontaneous Radiation Processes. *Phys. Rev.* **1954**, *93* (1), 99–110.
- (44) Tavis, M.; Cummings, F. W. The Exact Solution of N Two Level Systems Interacting with a Single Mode, Quantized Radiation Field. *Phys. Lett. A* **1967**, *25*, 714–715.
- (45) Garraway, B. M. The Dicke Model in Quantum Optics: Dicke Model Revisited. *Philos. Trans. R. Soc., A* **2011**, *369*, 1137–1155.
- (46) Bricks, J. L.; Slominskii, Y. L.; Panas, I. D.; Demchenko, A. P. Fluorescent J-Aggregates of Cyanine Dyes: Basic Research and Applications Review. *Methods Appl. Fluoresc.* **2018**, *6*, 12001.

(47) Kirstein, S.; Daehne, S. J-Aggregates of Amphiphilic Cyanine Dyes: Self-Organization of Artificial Light Harvesting Complexes. *Int. J. Photoenergy* **2006**, *2006*, 1–21.

(48) Chen, X.; Chen, Y.-H.; Qin, J.; Zhao, D.; Ding, B.; Blaikie, R. J.; Qiu, M. Mode Modification of Plasmonic Gap Resonances Induced by Strong Coupling with Molecular Excitons. *Nano Lett.* **2017**, *17*, 3246–3251.

(49) *J-Aggregates*; Kobayashi, Y., Ed.; World Scientific: Singapore, 1996.

(50) *J-Aggregates*; Kobayashi, T., Ed.; World Scientific: Singapore, 2012; Vol. 2.

(51) Balci, S.; Kucukoz, B.; Balci, O.; Karatay, A.; Kocabas, C.; Yaglioglu, G. Tunable Plexcitonic Nanoparticles: A Model System for Studying Plasmon-Exciton Interaction from the Weak to the Ultrastrong Coupling Regime. *ACS Photonics* **2016**, *3*, 2010–2016.

(52) DeLacy, B. G.; Miller, O. D.; Hsu, C. W.; Zander, Z.; Lacey, S.; Yagloski, R.; Fountain, A. W.; Valdes, E.; Anquillare, E.; Soljačić, M.; et al. Coherent Plasmon-Exciton Coupling in Silver Platelet-J-Aggregate Nanocomposites. *Nano Lett.* **2015**, *15*, 2588–2593.

(53) Fales, A. M.; Norton, S. J.; Crawford, B. M.; DeLacy, B. G.; Vo-Dinh, T. Fano Resonance in a Gold Nanosphere with a J-Aggregate Coating. *Phys. Chem. Chem. Phys.* **2015**, *17*, 24931–24936.

(54) Das, K.; Hazra, B.; Chandra, M. Exploring the Coherent Interaction in a Hybrid System of Hollow Gold Nanoprisms and Cyanine Dye J-Aggregates: Role of Plasmon-Hybridization Mediated Local Electric-Field Enhancement. *Phys. Chem. Chem. Phys.* **2017**, *19*, 27997–28005.

(55) Nasr, C.; Hotchandani, S. Excited-State Behavior of Nile Blue H-Aggregates Bound to SiO₂ and SnO₂ Colloids. *Chem. Mater.* **2000**, *12*, 1529–1535.

(56) Patlolla, P. R.; Mallajosyula, S. S.; Datta, B. Template-Free Self-Assembly of Dimeric Dicarboxyanine Dyes. *ChemistrySelect* **2017**, *2*, 10709–10717.

(57) Rodarte, A. L.; Tao, A. R. Plasmon-Exciton Coupling between Metallic Nanoparticles and Dye Monomers. *J. Phys. Chem. C* **2017**, *121*, 3496–3502.

(58) Li, N.; Han, Z.; Huang, Y.; Liang, K.; Wang, X.; Wu, F.; Qi, X.; Shang, Y.; Yu, L.; Ding, B.; et al. Strong Plasmon-Exciton Coupling in Bimetallic Nanorings and Nanocuboids. *J. Mater. Chem. C* **2020**, *8*, 7672–7678.